SIAM J. SCI. COMPUT.
Vol. 35, No. 3, pp. B799–B819

ASYMPTOTIC-PRESERVING NUMERICAL SCHEMES FOR THE SEMICONDUCTOR BOLTZMANN EQUATION EFFICIENT IN THE HIGH FIELD REGIME*

SHI JIN† AND LI WANG‡

Abstract. We present asymptotic-preserving numerical schemes for the semiconductor Boltzmann equation efficient in the high field regime. A major challenge in this regime is that there may be no explicit expression of the local equilibrium which is the main component of classical asymptotic-preserving schemes. Inspired by [F. Filbet and S. Jin, *J. Comput. Phys.*, 229 (2010), pp. 7625–7648] and [F. Filbet, J. Hu, and S. Jin, *Math. Model. Numer. Anal.*, 46 (2012), pp. 443–463], our idea is to penalize the stiff collision term with a classical Bhatnagar–Gross–Krook operator—which is not the local equilibrium in the high field limit—while treating the stiff force term implicitly with the spectral method. These schemes, despite being implicit, can be inverted easily with a stability independent of the physically small parameter. We design these schemes for both nondegenerate and degenerate cases and show their asymptotic properties. We present several numerical examples to validate the efficiency, accuracy, and asymptotic properties of these schemes.

Key words. Boltzmann equation, semiconductor, high field limit, asymptotic-preserving schemes

AMS subject classifications. 82C40, 82C80, 82D10, 82D37

DOI. 10.1137/120886534

1. Introduction.

In the semiconductor kinetic theory, the semiclassical evolution of the electron distribution function $f(t,x,v)$, in the parabolic band approximation, solves the kinetic equation

$$\partial_t f + v\cdot\nabla_x f - \frac{q}{m_e}E\cdot\nabla_v f = \mathcal{Q}(f), \quad t>0, x\in\mathbb{R}^{d_x}, v\in\mathbb{R}^{d_v}, \tag{1.1}$$

where q and m_e are positive elementary charge and effective mass of electrons and $E(t,x)$ is the electric field. The collision operator $\mathcal{Q}$ can be decomposed into three parts,

$$\mathcal{Q} = \mathcal{Q}_{el} + \mathcal{Q}_{inel} + \mathcal{Q}_{ee}, \tag{1.2}$$

where $\mathcal{Q}_{el}$ and $\mathcal{Q}_{inel}$ describe the interactions between the electrons and the lattice imperfections, with the first one caused by ionized impurities and elastic part of the phonon collisions (or crystal vibrations) and the second one by inelastic part of the phonon collisions. $\mathcal{Q}_{ee}$ characterizes the correlations between electrons themselves. For low electron densities, the general form of $\mathcal{Q}$ is [25]

$$\mathcal{Q}(f) = \int_{\mathbb{R}^{d_v}} \big(s(v',v)f(t,x,v') - s(v,v')f(t,x,v)\big)dv', \tag{1.3}$$

*Submitted to the journal's Computational Methods in Science and Engineering section July 31, 2012; accepted for publication (in revised form) April 15, 2013; published electronically June 27, 2013. This research was partly supported by NSF grant DMS-1114546 and NSF RNMS grant DMS-1107291.

http://www.siam.org/journals/sisc/35-3/88653.html

†Department of Mathematics, Institute of Natural Sciences, and Ministry of Education Key Laboratory of Scientific and Engineering Computing, Shanghai Jiao Tong University, Shanghai 20040, China, and Department of Mathematics, University of Wisconsin–Madison, Madison, WI 53706 (jin@math.wisc.edu). This author's work was supported by a Vilas Associate award from the University of Wisconsin–Madison.

‡Department of Mathematics, University of Michigan, Ann Arbor, MI 48104 (wangbao@umich.edu).

where s is the transition probability depending on the specific scattering mechanism described above, and satisfies the principle of detailed balance

$$s(v', v)M(v') = s(v, v')M(v), \tag{1.4}$$

where

$$M(v) = \left(\frac{2\pi K_B T}{m_e}\right)^{-\frac{d_v}{2}} e^{-\frac{v^2}{2v_{th}^2}} \tag{1.5}$$

is the Maxwellian, v_{th} is the thermal velocity related to the lattice temperature T through $v_{th}^2 = \frac{K_B T}{m_e}$, and K_B is the Boltzmann constant. The null space of $\mathcal{Q}$ in (1.3) is spaned by the Maxwellian (1.5).

When the electron density is high, one should take Pauli's exclusion principle into account, and the collision operator $\mathcal{Q}$ becomes

$$\mathcal{Q}_{deg}(f) = \int_{\mathbb{R}^{N_v}} \big(s(v', v)f'(1-f) - s(v, v')f(1-f')\big)dv', \tag{1.6}$$

which is referred to as the degenerate case. Here the transition probability s again satisfies the detailed balance (1.4) [27], and f and f' are shorthand notation for $f(t, x, v)$ and $f(t, x, v')$, respectively.

In principle, the electric field is produced self-consistently by the electrons moving in a fixed ion background with doping profile $h(x)$ through

$$\nabla_x(\varepsilon(x)\nabla_x\Phi) = \rho(x) - h(x), \qquad E = -\nabla_x\Phi, \tag{1.7}$$

where $\rho(x)$ is the electron density, Φ is the electrostatic potential, and $\varepsilon(x)$ is the permittivity of the material.

The numerical computation of electron transport in semiconductors through the Boltzmann equation (1.1) is usually too costly for practical purposes since it involves the resolution of a problem rested on seven-dimensional time and space. Several macroscopic models based on the diffusion approximation were derived. The classical drift-diffusion [33] model was introduced, with the assumption that all the scatterings in $\mathcal{Q}$ are strong and that the electron temperature relaxes to the lattice temperature at the microscopic time scale. The connection between the Boltzmann equation and drift-diffusion models has been well understood physically and mathematically [18, 28]. The case of the Fermi–Dirac statistics was investigated in [18] as well. However, in most situations, the momentum relaxation occurs much faster than temperature relaxation, resulting in an intermediate state at which the electrons have reached a local equilibrium with a different temperature than the lattice temperature. The time evolution of this state is described by the energy-transport model, which is a system of diffusion equations for the electron density and energy. This model can be viewed as an augmented drift-diffusion model and is derived asymptotically under the scaling that both the elastic $\mathcal{Q}_{el}$ and electron-electron $\mathcal{Q}_{ee}$ collisions are dominant [4]. Another model is the spherical harmonic expansion model, which is obtained based on the observation that in some cases the electron-electron collision cannot constitute one of the dominant scattering mechanisms [30, 31]. This model, the only dominant collision mechanism of which is $\mathcal{Q}_{el}$, can be considered as a diffusion equation in the extended space: position and energy. In fact, the energy-transport model was usually derived through the spherical harmonic expansion model by taking the limit on the scaled electron-electron collision mean free path [10]. See also [11] for the new

and simpler derivation of the energy-transport model directly through the Boltzmann equation. (Abdallah and Degond) [3] outline a hierarchy between various macroscopic models as well as show the macroscopic limit that links the two successive steps within the hierarchy.

However, due to the rapid progress in miniaturization of semiconductor devices, the standard drift-diffusion models break down in some regime of hot electron transport. This regime concerns the physical situations where both the electric effects and collisions are dominant, which is called the high field regime. After rescaling of the variables, (1.1) can be written as

$$\partial_t f + v \cdot \nabla_x f - \frac{1}{\epsilon} E \cdot \nabla_v f = \frac{1}{\epsilon} \mathcal{Q}(f), \quad t > 0, \quad x \in \mathbb{R}^{d_x}, \quad v \in \mathbb{R}^{d_v}, \tag{1.8}$$

where ϵ is the ratio between the mean free path and the typical length scale. It was first studied by Frosali and others [17, 16] and later by Poupaud [29] for the nondegenerate case, where the limiting equation is a linear convection equation for the mass density with the convection proportional to the electric field. It also gives a necessary condition for the limit equation to embrace a unique solution, while if such a condition is not satisfied, a traveling wave solution will exist, which is the so-called runaway phenomenon. When the electrostatic potential is obtained through the Poisson equation, Cercignani, Gamba, and Levermore [7] derive the high field limit for the Bhatnagar–Gross–Krook (BGK) type collision and also reveal the boundary layer behavior when bounded domain is considered. The high field asymptotic for the degenerate case was carried out in [1], where the limit equation is a nonlinear convection equation for the macroscopic density which has a local-in-time regular solution. It was revisited in [2], where the convergence to entropy solutions and existence of shock profiles for the limit nonlinear conservation law were considered.

Considerable literature has been devoted to the design of efficient and accurate numerical methods for (1.1), such as [20, 5, 6, 8, 13], to name just a few. These schemes become inefficient in the high field regime. Only recently, schemes efficient in the high field regime started to emerge [24, 9] in the framework of a symptotic-preserving (AP) schemes. The AP schemes are efficient in the asymptotic regime since the scheme preserves a discrete analogue of the asymptotic limit, so one does not need to numerically resolve the small scale of ϵ. It is often equipped with suitable time integrators in order to efficiently handle the numerical stiffness of the problem [21]. See a recent review on AP schemes [22].

In this paper, we are interested in designing AP schemes for the Boltzmann equation of type (1.8) with high field scaling. So far the only AP schemes for the high field regime were those developed in [24, 9], in which $\mathcal{Q}(f)$ is the Fokker–Planck operator. In this case one can combine the forcing term and the collision term into a divergence form, which cannot be done for other nonlocal collision operators to be studied in this paper.

As one can see, when ϵ is small, two terms of (1.8) become stiff and explicit schemes are subject to severe stability constraints. Implicit schemes allow larger time steps and mesh sizes, but it is usually expensive due to the prohibitive computational cost required by inverting a large algebraic system, even in the nondegenerate case where the collision operator is linear. Another remarkable difficulty is that there is no specific form of the *local equilibrium* M_h in the high field regime, which makes the modern AP methods such as [9, 12, 34]—all need the specific form of the local equilibrium—very hard to implement. To overcome the first difficulty, we follow the idea in [15] by penalizing the nonsymmetric stiff term with a BGK operator,

which is much easier to treat implicitly. To overcome the second difficulty, inspired by the observation in [14] that one needs, not use the exact local equilibrium as a penalization but rather a "good" approximation of it might be enough, we only penalize the collision term with a classical BGK operator with the Maxwellian defined in (1.5) instead of the real local equilibrium for the high field limit, which may not be available, and leave the stiff force term alone implicitly.

The rest of the paper is organized as follows. In the next section we give a brief review of the scalings in the high field regime and the corresponding macroscopic limit. Section 3 is devoted to the new schemes, as well as the study of their asymptotic properties. We consider three cases: the nondegenerate isotropic case, the nondegenerate anisotropic case, and the degenerate case. Then we present several numerical examples to test the efficiency, accuracy and asymptotic properties of the schemes in section 4. At last, some concluding remarks are given in section 5.

2. Scalings and the high field limit. Since the transition probability in (1.3) satisfies the detailed balance principle, it is convenient to introduce a new function

$$\phi(v,v') = \frac{s(v',v)}{M(v)} \quad \text{so that } \phi(v,v') = \phi(v',v). \tag{2.1}$$

Then the collision $\mathcal{Q}$ reads

$$\mathcal{Q}(f) = \int_{\mathbb{R}^{d_v}} \phi(v,v')\big(M(v)f(t,x,v') - M(v')f(t,x,v)\big)dv' = \mathcal{Q}^+(f) - \mathcal{Q}^-(f). \tag{2.2}$$

The degenerate case $\mathcal{Q}_{deg}$ can be reformulated in the same manner:

$$\begin{aligned}\mathcal{Q}_{deg}(f)(t,x,v) = \int_{\mathbb{R}^{d_v}} \phi(v',v)\Big(&M(v)f(t,x,v')\big(1-f(t,x,v)\big)\\ &- M(v')f(t,x,v)\big(1-f(t,x,v')\big)\Big)dv'\\ = \mathcal{Q}^+_{deg}(f) &- \mathcal{Q}^-_{deg}(f).\end{aligned} \tag{2.3}$$

Following [29], and also Chapter 2 in [25], we introduce the rescaled variables,

$$\tilde{x} = \frac{x}{L}, \quad \tilde{t} = \frac{t}{\Gamma}, \quad \tilde{v} = \frac{v}{v_{th}},$$

where L and T are reference length and time. By the dimension argument, the collision term should be proportional to the reciprocal of a characteristic time, thus we define an average relaxation time τ and the rescaled collision $\tilde{\mathcal{Q}}$,

$$\frac{1}{\tau} = \mathcal{Q}^+(M), \qquad \tilde{\mathcal{Q}} = \tau\mathcal{Q}.$$

Note here that for the degenerate case the definition of τ is a bit different but similar. The mean free path now can be defined as $l = \tau v_{th}$. Next define the thermal voltage U_{th} and the rescaled electric field $\tilde{E}$ as

$$U_{th} = \frac{m_e v_{th}^2}{q}, \qquad \tilde{E} = \frac{E}{E_0},$$

where E_0 is a reference field. Then the Boltzmann equation (1.1) takes the form

$$\frac{\tau}{\Gamma}\,\partial_{\tilde{t}} f + \frac{\tau v_{th}}{L}\,\tilde{v}\cdot\nabla_{\tilde{x}} f - \frac{\tau v_{th}}{U_{th}}E_0\,\tilde{E}\cdot\nabla_{\tilde{v}} f = \tilde{\mathcal{Q}}. \tag{2.4}$$

Now we introduce the dimensionless parameter $\epsilon = \frac{l}{L}$ and consider the high field scalings

$$E_0 = \frac{U_{th}}{l}, \quad \Gamma = \frac{\tau}{\epsilon};$$

(2.4) becomes

$$\partial_t f + v \cdot \nabla_x f - \frac{1}{\epsilon} E \cdot \nabla_v f = \frac{1}{\epsilon} \mathcal{Q}(f), \tag{2.5}$$

where we have dropped the tilde for convenience.

2.1. The high field limit: The nondegenerate case. In (2.5), when ϵ vanishes, the limiting equation is a linear convection equation for the macroscopic particle density with a convection proportional to the scaled electric field. That is,

$$f(t,x,v) \to \rho(t,x) F_{E(t,x)}(v),$$

where $F_{E(t,x)}(v)$ is the solution to

$$\int_{\mathbb{R}^{d_v}} F_E(v) dv = 1, \quad E \cdot \nabla_v F_E + \mathcal{Q}(F_E) = 0, \quad F_E \geq 0. \tag{2.6}$$

while the equation for the macroscopic density ρ is obtained by integrating (2.5) w.r.t. v,

$$\partial_t \rho(t,x) + \int_{\mathbb{R}^{d_v}} v \cdot \nabla_x f = 0,$$

and then passing to the limit to get

$$\partial_t \rho(t,x) + \nabla_x \cdot (\rho(t,x) \sigma(E(t,x))) = 0, \quad \sigma(E) = \int_{\mathbb{R}^{d_v}} v F_E(v) dv. \tag{2.7}$$

Not all $\mathcal{Q}$ gives a unique solution of (2.6). Poupaud [29] gave a criterion for the transition probability s in the following theorem.

THEOREM 2.1 (see [29]). *Assume that the collision cross section $\phi(v,v') > 0$ satisfies $\phi(v,v') \in W^{1,\infty}(\mathbb{R}^{2d_v})$; then the collision frequency*

$$\nu(v) = \int_{\mathbb{R}^{d_v}} s(v,v') dv' = \int_{\mathbb{R}^{d_v}} \phi(v,v') M(v') dv' \tag{2.8}$$

is bounded and positive. If it further satisfies

$$\int_0^\infty \nu(v + \eta E) d\eta = +\infty, \quad a.e., \tag{2.9}$$

and the initial data $f(0,x,v) = f^0(x,v)$ solves $E \cdot \nabla_v f^0(x,v) - \mathcal{Q}(f^0)(x,v) = 0$ a.e., then the solution to (2.5) converges to ρF_E in the following sense: $\exists$ a positive constant C_T that depends on the initial data such that for any time $t \leq T$, the inequality

$$\| f(t,\cdot,\cdot) - \rho(t,\cdot) F_{E(t,\cdot)}(\cdot) \|_{L^1(\mathbb{R}^{d_x} \times \mathbb{R}^{d_v})} \leq C_T \epsilon$$

holds.

Equation (2.7) together with (2.6) can be regarded as the first order approximation of (2.5) which resembles the hydrodynamic approximation of the Boltzmann equation by the Euler equations. Equation (2.7), which rules out all the diffusion effect, is nothing but Ohm's law. If one goes further to the second order approximation, a new drift diffusion equation can be derived, which again resembles the Navier–Stokes approximation of the Boltzmann equation.

Remark 2.2. The above result is obtained for the case where electrical field is given. The analytical result for the case when the electrical field is self-consistent through the Poisson equation is derived by Cercignani, Gamba, and Levermore in [7] only for the BGK collision operator, while for general collision it is still open.

2.2. The high field limit: The degenerate case. Assume B is either the Brillouin zone or the whole space $\mathbb{R}^{d_v}$. When sending ϵ to 0, f can no longer be decoupled into two functions with one depending on x and t and the other on v separately because of the nonlinearity of the collision operator; instead one has, under the hypothesis that $\phi \in W^{2,\infty}(B^2)$ and $\phi_0 \le \phi(v, v') \le \phi_1$ for some positive constant ϕ_0 and ϕ_1,

$$f \to F(\rho(t,x), E(t,x))(v),$$

where $F(\rho, E)(v)$ is the unique solution in space $D_E = \{F \in L^1(B);\ E\cdot\nabla_v F \in L^1(B)\}$ such that $0 \le F \le 1$ and

$$E \cdot \nabla_v F - \mathcal{Q}_{deg}(F) = 0, \quad \int_{\mathbb{R}^{d_v}} F(t,x,v)dv = \rho(t,x). \tag{2.10}$$

Moreover, the mapping

$$(\rho, E) \mapsto F(\rho, E) \tag{2.11}$$

from $\mathbb{R}^+ \times \mathbb{R}^{d_x}$ to $L^1(B)$ is C^2 differentiable. Then the macroscopic density ρ solves

$$\partial_t \rho(t,x) + \nabla_x \cdot \Big(j(\rho(t,x); E(t,x))\Big) = 0, \ \ \rho(0,x) = \int_{\mathbb{R}^{d_v}} f^0(x,v)dv, \tag{2.12}$$

where $j(\rho; E) = \int_{\mathbb{R}^{d_v}} vF(\rho, E)(v)dv$. This result was proved in [1] for a given $E(x) \in \mathbb{R}^{d_x}$ on the time intervals such that the limit solution is regular.

Remark 2.3. Although there is no such condition (2.9) to ensure the existence of the limit solution, the hypothesis that $\phi(v, v')$ should be uniformly bounded from below and above already implies it.

Remark 2.4. Due to the nonlinearity of the flux function in (2.12), only the existence and uniqueness of local-in-time regular solutions were available and shock might be generated later [2]. This is different from the nondegenerate case, where the limit equation (2.7) is linear in ρ, and thus a unique global in time solution exists.

3. A numerical scheme for the semiconductor Boltzmann equation. To design an AP method, one usually needs to treat the two stiff terms—the force term and the collision term—implicitly. However, this would bring new difficulties to invert the algebraic system originated by the nonsymmetric difference operator and the collision operator. In [24] and [9] when the collision is of the Fokker–Planck type, these two terms were combined and rewritten into one symmetric operator in velocity space. But unfortunately, this strategy cannot be implemented here because no symmetric combination of the two is available. Another remarkable difficulty is that

one cannot write the local equilibrium M_h in the high field limit explicitly, and thus we cannot use the existing AP method for the kinetic equation in the hydrodynamic regime [9], nor can we use the even-odd decomposition [23] because one cannot derive a "nonstiff" force term. Here we adopt the penalization idea introduced by Filbet and Jin [15]. In addition, inspired by the fact that functions that share the same conserved quantities with the exact local equilibrium can be used as candidates for penalty [14], we will only penalize the collision term by a BGK operator which conserves mass and treat the stiff force term implicitly by the spectral method. To better illustrate our idea, we begin with the simplest case, which is the so-called time relaxation model.

Here for simplicity we will explain our idea in the one-dimensional case. The generalization to the multidimensional case can be done in a straightforward manner simply using dimension-by-dimension discretization. Denote $f(x_l, v_m, t^n)$ by f^n_{lm}, where $0 \le l \le N_x$ and $0 \le m \le N_v$, and N_x and N_v are the numbers of mesh points in x and v directions, respectively.

3.1. The nondegenerate isotropic case. In the low density approximation, if one only considers the collisions with background impurities, the collision operator can be approximated by a linear relaxation time operator [7, 25],

$$\mathcal{Q} = \int Mf' - M'f dv' = M\rho - f, \tag{3.1}$$

which is the simplest case with $\phi(v', v) = 1$ in (2.2), and M is defined in (1.5). This is usually called the time-relaxation model. In this model, one can directly treat both stiff terms implicitly. The first order scheme reads

$$\frac{f^{n+1} - f^n}{\triangle t} + v \cdot \nabla_x f^n - \frac{1}{\epsilon} E \cdot \nabla_v f^{n+1} = \frac{1}{\epsilon}(M\rho^{n+1} - f^{n+1}), \tag{3.2}$$

and we use the spectral discretization for the stiff force term. The scheme can be implemented as follows:

- Step 1. Integrate (3.2) over v; note that the two stiff terms vanish, and one ends up with an explicit semidiscrete scheme for ρ^{n+1}:

$$\frac{\rho^{n+1} - \rho^n}{\triangle t} + \nabla_x \cdot \int_{\mathbb{R}^{d_v}} v f^n dv = 0.$$

  - Step 1.1. If the electrical field is given by (1.7), then solve it by any Poisson solver such as the spectral method to get E^{n+1}.
- Step 2. Approximate the transport term $v \cdot \nabla_x f^n$ in (3.2) by a nonoscillatory high-resolution shock-capturing method.
- Step 3. Use the spectral discretization for the stiff force term, i.e., (3.2) can be reformulated into

$$\left[1 + \frac{\triangle t}{\epsilon} - \frac{\triangle t}{\epsilon} E \cdot \nabla_v\right] f^{n+1} = f^n - \triangle t v \cdot \nabla_x f^n + \frac{\triangle t}{\epsilon} M\rho^{n+1};$$

  then take the discrete Fourier transform w.r.t. v on both sides, and one has

$$\left[1 + \frac{\triangle t}{\epsilon} - i\frac{\triangle t}{\epsilon} E \cdot k\right] \hat{f}^{n+1} = \mathscr{F}\left(f^n - \triangle t v \cdot \nabla_x f^n + \frac{\triangle t}{\epsilon} M\rho^{n+1}\right), \tag{3.3}$$

  where $\hat{f}$ and $\mathscr{F}(f)$ denote the discrete Fourier transform of f w.r.t. v.
- Step 4. Use the inverse Fourier transform on $\hat{f}^{n+1}$ to get f^{n+1}.

Remark 3.1. Although the force term $\frac{E}{\epsilon}\cdot\nabla_v f$ contains a derivative, which looks "more stiff" than the collision term, just treating it implicitly and leaving the collision explicit will not have the desired stability property. This can be seen from the simple Fourier analysis on the toy model

$$f_t + \frac{E}{\epsilon} f_v = -\frac{1}{\epsilon} f \tag{3.4}$$

with the discretization

$$\frac{f^{n+1}-f^n}{\triangle t} + \frac{E}{\epsilon}\partial_v f^{n+1} = -\frac{1}{\epsilon} f^n,$$

where $f^n(v)$ denotes $f(t^n, v)$. Applying the Fourier transform on $f^n(v)$ w.r.t. v to get $\hat{f}^n(k)$, one then has

$$\left|\hat{f}^{n+1}(k)\right|^2 = \frac{\left(1-\frac{\triangle t}{\epsilon}\right)^2}{1+\left(\frac{\triangle t}{\epsilon}E\cdot k\right)^2}\left|\hat{f}^n(k)\right|^2;$$

note that for stability the coefficient on the right-hand side needs to be less than one for all values of k, that is, $\frac{\triangle t}{\epsilon} < 2$, and thus $\triangle t$ must be dependent of ϵ.

The scheme has the following AP property.

PROPOSITION 3.2. *Assume all functions are smooth. Let*

$$\| f^n(x,\cdot)\|_{L^2(\mathbb{R}^{d_v})} = \sqrt{\int_{\mathbb{R}^{d_v}} f(t^n,x,v)^2 dv}. \tag{3.5}$$

Then in the regime $\triangle t \gg \epsilon$ we have

$$\|f^n - M_h^n\|_{L^2(\mathbb{R}^{d_v})} \le \alpha^n \|f^0 - M_h^0\|_{L^2(\mathbb{R}^{d_v})} + O(\epsilon) \quad \text{with } \alpha < 1 \text{ uniformly in } \epsilon, \tag{3.6}$$

where $M_h^n = \rho^n F_E$ is the local equilibrium in the high field regime with F_E being the solution to the limit equation (2.6) *with $\mathcal{Q} = \rho M - f$.*

Proof. Since M_h^{n+1} satisfies $-E\cdot\nabla_v M_h^{n+1} = \mathcal{Q}(M_h^{n+1}) = \rho^{n+1}M - M_h^{n+1}$, a simple manipulation of scheme (3.2) gives

$$\begin{aligned}\left(1+\frac{\triangle t}{\epsilon} - \frac{\triangle t}{\epsilon}E\cdot\nabla_v\right)(f^{n+1}-M_h^{n+1}) \\ = (f^n - M_h^n) - (M_h^{n+1} - M_h^n) - \triangle t v\cdot\nabla_x f^n.\end{aligned} \tag{3.7}$$

Now taking the Fourier transform w.r.t. v on both sides, (3.7) reformulates to

$$\begin{aligned}&\hat{f}^{n+1} - \hat{M}_h^{n+1} \\ &\quad = G\left[(\hat{f}^n - \hat{M}_h^n) - (\hat{M}_h^{n+1} - \hat{M}_h^n) - \triangle t\mathscr{F}(v\cdot\nabla_x f^n)\right],\end{aligned} \tag{3.8}$$

where

$$G = \frac{1}{1+\frac{\triangle t}{\epsilon} - i\frac{\triangle t}{\epsilon}E\cdot k}. \tag{3.9}$$

Taking the L^2 norm on both sides, one has by the Minkowski inequality

$$\begin{aligned}&\| \hat{f}^{n+1} - \hat{M}_h^{n+1}\|_{L^2} \\ &\quad \le \| G(\hat{f}^n - \hat{M}_h^n)\|_{L^2} + \left\| G\left((\hat{M}_h^{n+1} - \hat{M}_h^n) + \triangle t\mathscr{F}(v\cdot\nabla_x f^n)\right)\right\|_{L^2}.\end{aligned} \tag{3.10}$$

By the smoothness assumption $|\hat{M}_h^{n+1} - \hat{M}_h^n| \le C_1 \triangle t \hat{M}_h$ and $\|G \triangle t\|_{L^\infty} \le C_2\epsilon$ for $\triangle t \gg \epsilon$, where C_1 and C_2 are two constants independent of $\triangle t$ and ϵ. Then (3.10) becomes

$$\| \hat{f}^{n+1} - \hat{M}_h^{n+1} \|_{L^2} \le \| G(\hat{f}^n - \hat{M}_h^n) \|_{L^2} + C\epsilon.$$

Since $\| G \|_{L^\infty} \le \alpha < 1$ uniformly in ϵ for $\triangle t \gg \epsilon$, applying Parseval's identity, one has

$$\|f^{n+1} - M_h^{n+1}\|_{L^2(\mathbb{R}^{d_v})} \le \alpha \|f^n - M_h^n\|_{L^2(\mathbb{R}^{d_v})} + O(\epsilon).$$

This leads to (3.6). ∎

3.2. The nondegenerate anisotropic case. This section is devoted to the non-degenerate anisotropic case. Recall that the collision operator takes the form

$$\mathcal{Q}(f) = \int_{\mathbb{R}^{N_v}} \phi(v, v') \big(M(v) f(t, x, v') - M(v') f(t, x, v)\big) dv' = \mathcal{Q}^+(f) - \nu(v) f. \tag{3.11}$$

Although $\mathcal{Q}$ is linear in f, due to the non-symmetric nature of the transition probability $s(v', v)$, treating it implicitly as we did in the last section will make it difficult to invert, especially in higher dimensions. To overcome this difficulty, we adopt the idea introduced by Filbet and Jin in [15] by penalizing the collision term with a BGK operator, the simple structure of which makes it easy to be treated implicitly. Thus the first order scheme reads

$$\frac{f^{n+1} - f^n}{\triangle t} + v \cdot \nabla_x f^n - \frac{1}{\epsilon} E \cdot \nabla_v f^{n+1} = \frac{1}{\epsilon} \mathcal{Q}(f^n) - \frac{\lambda}{\epsilon}(\rho^n M - f^n) + \frac{\lambda}{\epsilon}(\rho^{n+1} M - f^{n+1}), \tag{3.12}$$

where M is the dimensionless form of (1.5)

$$M(v) = \frac{1}{(2\pi)^{\frac{d_v}{2}}} e^{-\frac{v^2}{2}}. \tag{3.13}$$

Then (3.12) has the similar implicit structure as (3.2), and thus one can solve it with the steps introduced in section 3.1, yielding a scheme that is implicit but can be implemented explicitly.

Notice that in [15], the penalty is the local equilibrium of the collision operator, which will drive f to the right Maxwellian if treated implicitly. However, as mentioned, there is no explicit form of the "high field equilibrium" which is the solution to $E \cdot \nabla_v f = \mathcal{Q}(f)$, so we instead penalize the equation with the equilibrium ρM of the collision term $\mathcal{Q}(f)$, and this will indeed force f to the right local equilibrium with the following proposition. The cost of this "wrong Maxwellian" penalty is the extra $\triangle t$ error in (3.14). This was observed in [14], where the authors use the classical Maxwellian instead of the quantum one to penalize the quantum Boltzmann collision operator and get a similar asymptotic property.

PROPOSITION 3.3. *In* (3.12)*, if* $\mathcal{Q}$ *takes the form of* (3.1) *and* $\lambda > \frac{1}{2}$*, then*

$$\|f^n - M_h^n\|_{L^2(\mathbb{R}^{d_v})} \le \alpha^n \|f^0 - M_h^0\|_{L^2(\mathbb{R}^{d_v})} + O(\epsilon + \triangle t) \quad \textit{with } \alpha < 1, \tag{3.14}$$

where $M_h^n = \rho^n F_E$ *is the local equilibrium in the high field regime, with* F_E *being the solution to the limit equation* (2.6) *with* $\mathcal{Q}$ *defined in* (3.1)*.*

The proof is very similar to the one for Proposition 3.6 in the next section and is omitted here.

Remark 3.4 (choice of λ). For the general collision (3.11), λ serves as some appropriate approximation of $\nabla\mathcal{Q}(M)$. In practice, we choose $\lambda > \max_v \nu(v)$ for positivity concern [34], where ν is the collision frequency defined in (2.8).

Remark 3.5. This method can be easily extended to the case with a nonparabolic energy diagram such as Kane's model [5, 6, 8] since the convection term is treated explicitly.

3.3. The degenerate case. When the quantum effect is taken into account, the collision operator becomes nonlinear. Nevertheless, this can be dealt with in the same way as in section 3.2 at the same cost. Again inspired by [14], we use the classical Boltzmann distribution instead of the Fermi–Dirac distribution (3.16) as the penalty to avoid the complicated nonlinear solver for the Fermi energy in (3.16) from mass density ρ; otherwise such nonlinear solver should be used at every time step and grid point, which is very time-consuming. Since the $\triangle t$ error will be inevitable in the asymptotic property, as we have seen in the last section, this change of penalty will only introduce the new error of $O(\triangle t)$. Similar to (3.12), the first order scheme takes the form

(3.15)
$$\frac{f^{n+1}-f^n}{\triangle t}+v\cdot\nabla_x f^n-\frac{1}{\epsilon}E\cdot\nabla_v f^{n+1}=\frac{1}{\epsilon}\mathcal{Q}_{deg}(f^n)-\frac{\lambda}{\epsilon}(\rho^n M-f^n)+\frac{\lambda}{\epsilon}(\rho^{n+1}M-f^{n+1}),$$

where $\mathcal{Q}_{deg}$ is defined in (1.6) and M is the same as (3.13). In practice, similar to Remark 3.4, λ is chosen to be $\max_v \int_{\mathbb{R}^{d_v}} \phi(v',v)M(v')(1-f(v'))dv'$.

Because of the nonlinearity of $\mathcal{Q}_{deg}$, it is not easy to check the asymptotic property analytically. Instead we check it for the case where $\mathcal{Q}_{deg}$ is replaced by the "quantum BGK" operator $M_{FD}-f$ in the following proposition. Here M_{FD} is the Fermi–Dirac distribution and serves as the base for the null space of $\mathcal{Q}_{deg}$. It takes the form

$$M_{FD}=\frac{1}{1+e^{\frac{m_e v^2}{2K_BT}-\frac{\mu}{K_BT}}}, \tag{3.16}$$

where T is the lattice temperature and μ is the electron Fermi energy.

PROPOSITION 3.6. *Assume the solutions are smooth. If $\lambda > \frac{1}{2}$, then the scheme* (3.15) *with $\mathcal{Q}_{deg}$ replaced by $M_{FD}-f$ has the asymptotic property*

$$\|f^n-M_{qh}^n\|_{L^2(\mathbb{R}^{d_v})}\le\alpha^n\|f^0-M_{qh}^0\|_{L^2(\mathbb{R}^{d_v})}+O(\epsilon+\triangle t) \tag{3.17}$$

with $0<\alpha<1$, where M_{qh} is the solution to the high field limit equation with $\mathcal{Q}_{deg}(f)=M_{FD}-f$:

$$-E\cdot\nabla_v M_{qh}=M_{FD}-M_{qh},\quad \int_{\mathbb{R}^{d_v}}M_{qh}dv=\int_{\mathbb{R}^{d_v}}f dv=\int_{\mathbb{R}^{d_v}}M_{FD}dv=\rho. \tag{3.18}$$

Proof. Since M_{qh} satisfies $-E\cdot\nabla_v M_{qh}^{n+1}=M_{FD}^{n+1}-M_{qh}^{n+1}$, the scheme (3.15) becomes

$$\begin{aligned}\left(1+\frac{\lambda\triangle t}{\epsilon}-\frac{\triangle t}{\epsilon}E\cdot\nabla_v\right)(f^{n+1}-M_{qh}^{n+1})&\\ =\left(1+\frac{(\lambda-1)\triangle t}{\epsilon}\right)(f^n-M_{qh}^n)-\left(1+\frac{(\lambda-1)\triangle t}{\epsilon}\right)(M_{qh}^{n+1}-M_{qh}^n)&\\ +\ \frac{\lambda\triangle t}{\epsilon}(\rho^{n+1}-\rho^n)M-\frac{\triangle t}{\epsilon}(M_{FD}^{n+1}-M_{FD}^n)-\triangle t v\cdot\nabla_x f^n.&\end{aligned} \tag{3.19}$$

After taking the Fourier transform w.r.t. v on both sides, it reformulates to

(3.20)

$$\begin{aligned}
&\hat{f}^{n+1} - \hat{M}_{qh}^{n+1} \\
&\quad = \frac{1+\frac{(\lambda-1)\triangle t}{\epsilon}}{1+\frac{\lambda\triangle t}{\epsilon}-i\frac{\triangle t}{\epsilon}E\cdot k}\big(\hat{f}^n - \hat{M}_{qh}^n\big) \\
&\qquad - \frac{1+\frac{(\lambda-1)\triangle t}{\epsilon}}{1+\frac{\lambda\triangle t}{\epsilon}-i\frac{\triangle t}{\epsilon}E\cdot k}\big(\hat{M}_{qh}^{n+1} - \hat{M}_{qh}^n\big) + \frac{\frac{\lambda\triangle t}{\epsilon}}{1+\frac{\lambda\triangle t}{\epsilon}-i\frac{\triangle t}{\epsilon}E\cdot k}(\rho^{n+1}-\rho^n)\hat{M} \\
&\qquad - \frac{\frac{\triangle t}{\epsilon}}{1+\frac{\lambda\triangle t}{\epsilon}-i\frac{\triangle t}{\epsilon}E\cdot k}\big(\hat{M}_{FD}^{n+1} - \hat{M}_{FD}^n\big) - \frac{\triangle t}{1+\frac{\lambda\triangle t}{\epsilon}-i\frac{\triangle t}{\epsilon}E\cdot k}\mathscr{F}\big(v\cdot\nabla_x f^n\big).
\end{aligned}$$

Let

$$G_1 = \frac{1+\frac{(\lambda-1)\triangle t}{\epsilon}}{1+\frac{\lambda\triangle t}{\epsilon}-i\frac{\triangle t}{\epsilon}E\cdot k},$$

take the L^2 norm for (3.20), and apply the same procedure as in Proposition 3.2; then we have

$$\| \hat{f}^{n+1} - \hat{M}_{qh}^{n+1} \|_{L^2} \leq \ \| G_1 \|_{L^\infty} \| \hat{f}^n - \hat{M}_{qh}^n \|_{L^2} + O(\triangle t + \epsilon),$$

where the $O(\triangle t)$ terms come from the second, third, and fourth terms in (3.20) and form a major difference compared to (3.8). If $\lambda > \frac{1}{2}$, $\| G_1 \|_{L^\infty} \leq \alpha < 1$, the result (3.17) then follows. ∎

Remark 3.7. As already mentioned in [15], the AP scheme allows one to capture the leading order asymptotic solution (the so-called Euler limit). To capture the next order terms (the Navier–Stokes limit), one needs to use the mesh size and time step to be $o(\epsilon)$, namely, the resolved mesh.

Remark 3.8. To get a better asymptotic property than (3.14) and (3.17), we would like to extend the scheme to second order. Following the idea in [19], using the backward difference formula in time and the MUSCL scheme [32] in space, we have

$$\begin{aligned}
&\frac{3f^{n+1}-4f^n+f^{n-1}}{2\triangle t} + 2v\cdot\partial_x f^n - v\cdot\partial_x f^{n-1} + \frac{1}{\epsilon}E^{n+1}\cdot\partial_v f^{n+1} \\
&\quad = \frac{2}{\epsilon}\mathcal{Q}(f^n) - \frac{1}{\epsilon}\mathcal{Q}(f^{n-1}) - \frac{2\lambda}{\epsilon}(\rho^n M - f^n) + \frac{\lambda}{\epsilon}(\rho^{n-1}M - f^{n-1}) \\
&\qquad + \frac{\lambda}{\epsilon}(\rho^{n+1}M - f^{n+1}).
\end{aligned} \tag{3.21}$$

However, since the stiff terms contain a first derivative, it poses a very restrictive bound on λ for stability (here one condition we derived is $|\nabla_v \mathcal{Q}(f)| \leq \lambda \leq \min(3, \frac{5}{2} + \frac{\epsilon}{\triangle t})|\nabla_v \mathcal{Q}(f)|$), which might not be applicable in general cases. A better second order discretization in time is planned for a future work.

4. Numerical examples. In this section, we perform several numerical tests for the semiconductor Boltzmann equations with different collisions and in different asymptotic regimes. In the one-dimensional examples, we use the following settings unless otherwise specified. The computational domain for x and v is $[0, L_x] \times [-L_v, L_v] = [0,1] \times [-8,8]$ with $N_x = 128$ and $N_v = 32$. The time step is chosen

to be $\triangle t = \frac{\triangle x}{10}$ to satisfy the CFL condition $\triangle t \leq \frac{\triangle x}{\max_j |v_j|}$ in the transport part. Periodic boundary conditions in x will be used to avoid any difficulties that might be generated by the boundary. M is the absolute Maxwellian

$$M(v) = \frac{1}{\sqrt{2\pi}} e^{-\frac{v^2}{2}}. \tag{4.1}$$

The permittivity $\varepsilon(x)$ in the Poisson equation (1.7) is taken to be $\varepsilon(x) \equiv 1$.

4.1. The time relaxation model. We first test the numerical method presented in section 3.1 for the simplest time relaxation model (2.5) with (3.1). The initial condition is taken as

$$\rho^0(x) = \frac{\sqrt{2\pi}}{2}\left(2 + \cos(2\pi x)\right) \quad \text{and } f^0(x,v) = \rho^0(x) M(v), \tag{4.2}$$

which is not at the local equilibrium. The electric field $E(t,x)$ satisfies the Poisson equation (1.7) with the doping profile

$$h(x) = \frac{\int_0^{L_x} \rho(x)dx}{1.2611} e^{\cos(2\pi x)}. \tag{4.3}$$

We show the time evolution of the asymptotic error defined as

$$errorAP^n = \sum_{l,m} |E_l \cdot \nabla_v f_l^n + M\rho_l^n - f_{lm}^n| \triangle x \triangle v, \tag{4.4}$$

where the derivative w.r.t. v is calculated by the spectral method. Figure 4.1 gives the error with ϵ decreasing by $\frac{1}{10}$ each time, which shows that the asymptotic error is of order ϵ, thus verifying the results in Proposition 3.2. Here $\Delta t \sim O(10^{-3})$, so the scheme is asymptotically stable since it does not need to satisfy the constraint $\Delta t \leq C\epsilon$.

4.2. The nondegenerate anisotropic case. In this section, we consider the nondegenerate anisotropic case with collision cross section defined as

$$\phi(v, v') = 1 + e^{-(v-v')^2}, \tag{4.5}$$

and the initial condition is chosen the same as in (4.2).

• Asymptotic property. Consider fixed $E = 0.2$ at the moment. Figure 4.2 gives the relations between ϵ and the asymptotic error defined as

$$errorAP^n = \sum_{l,m} \left|E_l \cdot \nabla_v f_l^n + \mathcal{Q}(f)_{l,m}^n\right| \triangle x \triangle v, \tag{4.6}$$

where the derivative w.r.t. v is again calculated by the spectral method. The initial data is away from the equilibrium. It can be seen in Figure 4.2 that when ϵ is relatively large, the error is dominated by ϵ. However, when ϵ is small enough, the time step $\triangle t = 3.9063e-4$ will play a role so that the error will not decrease with ϵ. The first order scheme is better performed asymptotically than we expected in Proposition 3.3 as the error observed in Figure 4.2 is smaller than $O(\triangle t)$.

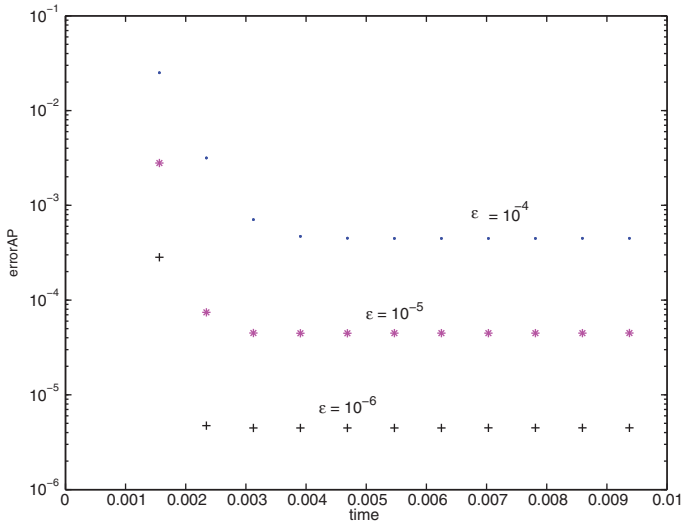

FIG. 4.1. *The time relaxation model coupled with the Poisson equation for the electric field. The time evolution of asymptotic error* (4.4) *for different* ϵ *with nonequilibrium initial data using the first order scheme in section* 3.1.

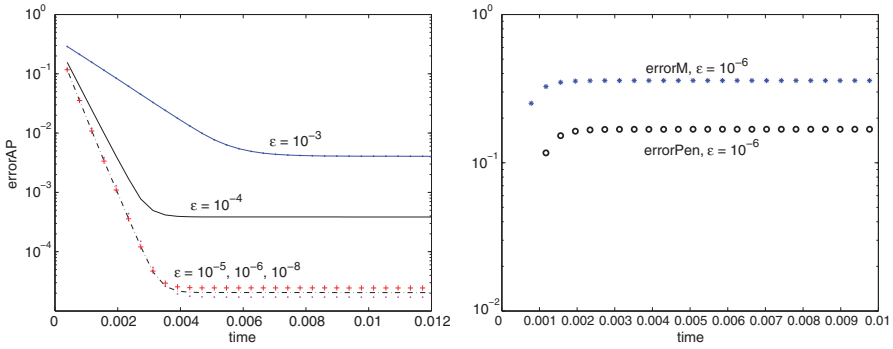

FIG. 4.2. *The nondegenerate anisotropic model with a fixed electrical field. The time evolution of asymptotic error* (4.6) *for different* ϵ *with nonequilibrium initial data (left) and a test of other errors* (4.7) *and* (4.8) *in comparison (right).*

To show that our scheme does not push f to the wrong Maxwellian, in Figure 4.2 we also plot the following two errors. One is defined as

$$errorPen^n = \sum_{l,m} \left| E_l \cdot \nabla_v f_l^n + \lambda(\rho_l^n M_m - f_{l,m}^n) \right| \triangle x \triangle v \tag{4.7}$$

to show that our penalization will not affect the asymptotic property. The other is the distance between f and the Maxwellian of the collision

$$errorM^n = \sum_{l,m} \left| f_{l,m}^n - \rho_l^n M_m \right| \triangle x \triangle v, \tag{4.8}$$

which shows that our implicit treatment of the stiff force term necessarily accounts for the right asymptotic limit. It is shown that both errors stay large when ϵ is small, which means f will not be driven to either above case when sending ϵ to 0.

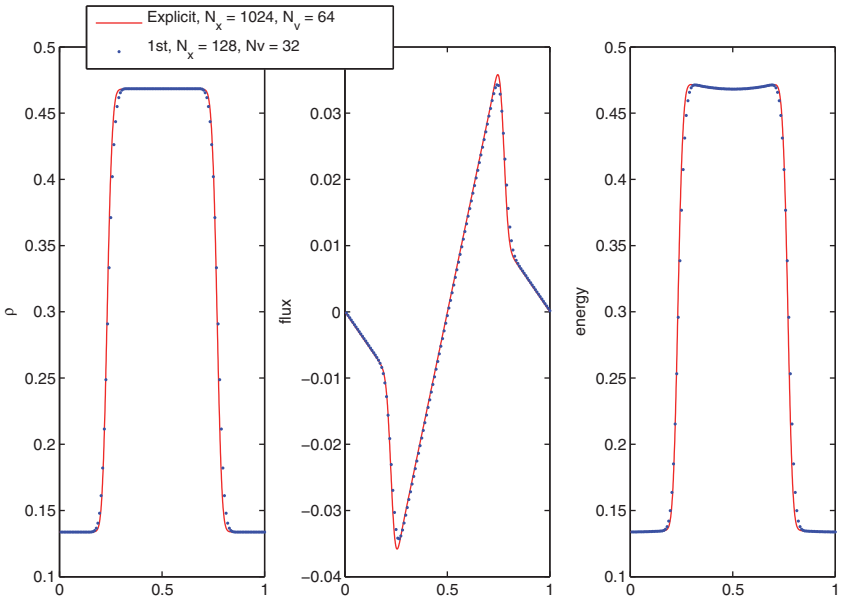

FIG. 4.3. *The plot of density, flux, and energy at time* $t = 0.2$ *of the anisotropic nondegenerate case with* (4.5) *with* E *obtained from the Poisson equation. The initial data is given in* (4.9).

• A piecewise constant initial data. Consider a piecewise constant initial data to test the efficiency of the method:

$$\begin{cases} (\rho_l, h_l) = (1/8, 1/2), & 0 \le x < 1/4; \\ (\rho_m, h_m) = (1/2, 1/8), & 1/4 \le x < 3/4; \\ (\rho_r, h_r) = (1/8, 1/2), & 3/4 \le x \le 1. \end{cases} \tag{4.9}$$

Initially $f^0(x,v) = \frac{\rho}{\sqrt{2\pi}} e^{-\frac{v^2}{2}}$ and let E be the solution of $-\nabla_x E = \rho - h$. Again the periodic boundary condition in x direction is applied. ϵ is fixed to be 10^{-3}. For a reference solution, we use the explicit second order Runge–Kutta discretization in time and the MUSCL scheme for space discretization, with $N_x = 1024$, $N_v = 64$, and $\triangle t = \min(\triangle x/10, \epsilon \triangle v)/4 = 2.4414e-05$.

Define the flux and energy as the first and second moments of f:

$$\text{flux} = \int_{-L_v}^{L_v} f v dv, \quad \text{energy} = \int_{-L_v}^{L_v} f v^2 dv. \tag{4.10}$$

From Figure 4.3, one sees a good match between our solution and the reference solution.

4.3. The degenerate case. In this section, we consider the degenerate case where the collision $\mathcal{Q}_{deg}$ is defined as (1.6).

• Asymptotic property. The initial condition is taken as

$$\rho^0(x) = \frac{\sqrt{2\pi}}{4}(2 + \cos(2\pi x)) \quad \text{and } f^0(x,v) = \rho^0(x) M(v) \tag{4.11}$$

to satisfy $0 \le f \le 1$. The electrical field E is obtained through the Poisson equation $-\nabla_x E = \rho - h$ with h given by (4.3). Again we compare the asymptotic error (4.6)

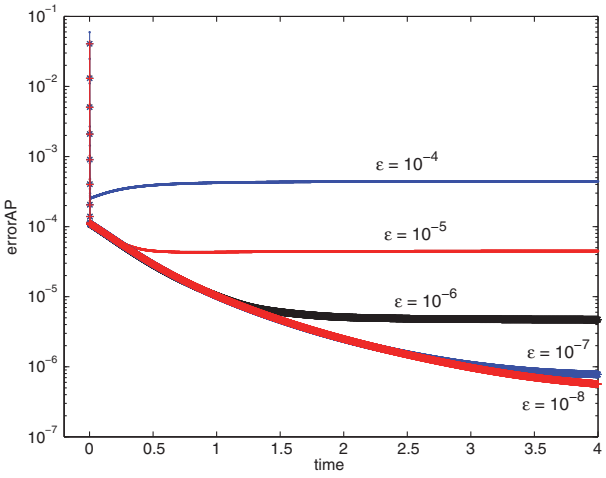

FIG. 4.4. *The degenerate isotropic model coupled with the Poisson equation. The time evolution of asymptotic error* (4.6) *with* $\mathcal{Q}$ *replaced by* $\mathcal{Q}_{deg}$ *for different* ϵ *with nonequilibrium initial data using the first order scheme in section* 3.1.

with $\mathcal{Q}$ replaced by $\mathcal{Q}_{deg}$ for different orders of ϵ. As in the nondegenerate anisotropic case, the error is first dominated by ϵ and then by $\triangle t^\beta$ when ϵ is small enough, which is the same as shown in section 3.3 (in section 3.3, β is shown to be 1, but numerically we get better results with $\beta > 1$); see Figure 4.4, where $\triangle t = 3.9063e - 4$.

- Mixing scales. To test the ability of our scheme for mixing scales, consider ϵ taking the following form:

$$\epsilon(x) = \begin{cases} \epsilon_0 + \frac{1}{2}(\tanh(5 - 10x) + \tanh(5 + 10x)) & x \le 0.3; \\ \epsilon_0 & x > 0.3, \end{cases} \tag{4.12}$$

where $\epsilon_0 = 0.001$ so that it contains both the kinetic and high field regimes; see Figure 4.5. The initial condition is taken to be

$$f^0(x) = \frac{1}{6}(2 + \sin(\pi x))e^{-\frac{1}{2}v^2}. \tag{4.13}$$

Consider the anisotropic scattering where $\phi(v, v')$ is taken as the same form as in (4.5). E is calculated through the Poisson equation (1.7) with h given by (4.3). We use the second order Runge–Kutta time discretization with the MUSCL scheme on a refined mesh to get the reference solution. Good agreements of these two solutions can be observed in Figure 4.6. We also plot the l^1 error in Figure 4.7 between these two solutions

$$error_g^n = \sum_{l,m} \left| (g_{AP})_{l,m}^n - (g_{ref})_{l,m}^n \right| \Delta v \Delta x, \tag{4.14}$$

where g represents the macroscopic quantities defined in (4.10), the subscript AP refers to the solution obtained by the AP scheme, and ref refers to the reference solution.

4.4. The electron-phonon interaction model. In this section, we consider a physically more realistic model, the electron-phonon interaction model, where the transition probability is

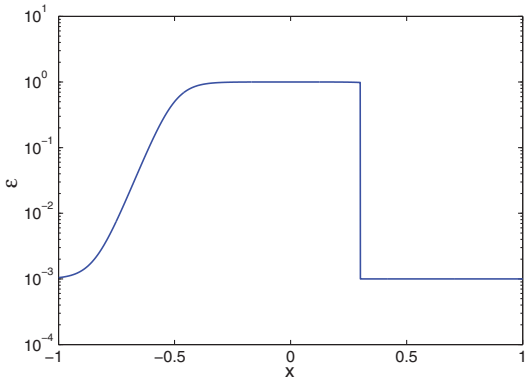

FIG. 4.5. ϵ *defined in* (4.12).

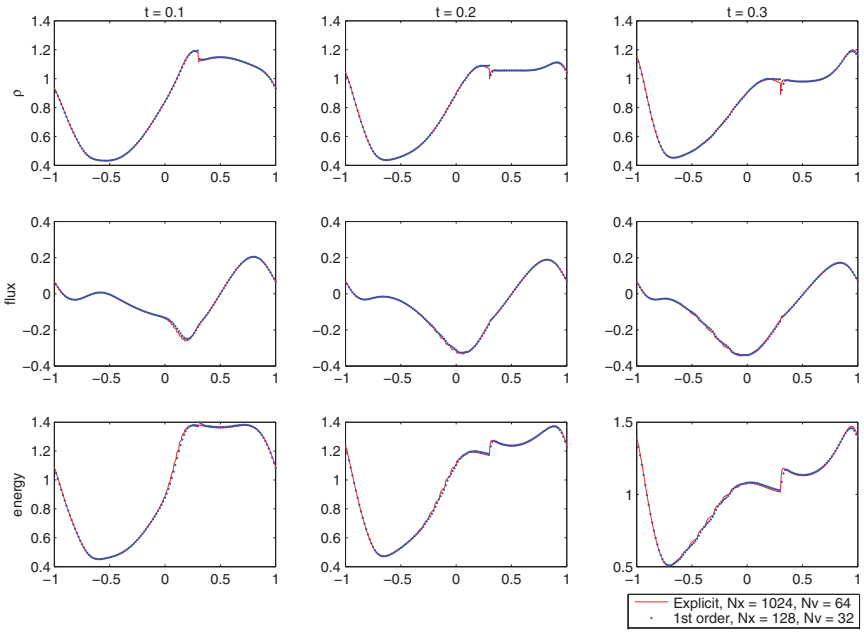

FIG. 4.6. *The degenerate anisotropic model coupled with the Poisson equation. Consider the mixing regimes with* ϵ *given in* (4.12). *Compare the first order scheme* (3.2) *on a coarse mesh with* $\Delta t = 0.0016$ *with an explicit method on refined mesh with* $\Delta t = 2.5e-05$. *We plot the macroscopic density, flux, and energy at different times.*

$$s(v,v') = K_0\delta\left(\frac{v'^2}{2} - \frac{v^2}{2}\right) + K\left[(n_q+1)\delta\left(\frac{v'^2}{2} - \frac{v^2}{2} + \hbar\omega_p\right) + n_q\delta\left(\frac{v'^2}{2} - \frac{v^2}{2} - \hbar\omega_p\right)\right], \tag{4.15}$$

and n_q given by $n_q = 1/e^{\frac{\hbar\omega_p}{K_B T_L}} - 1$ is the occupation number of phonons. Here $\hbar$ is the planck constant, K_B is the Boltzmann constant, ω_p is the constant phonon frequency, T_L is the lattice temperature, and K and K_0 are two constants for the material.

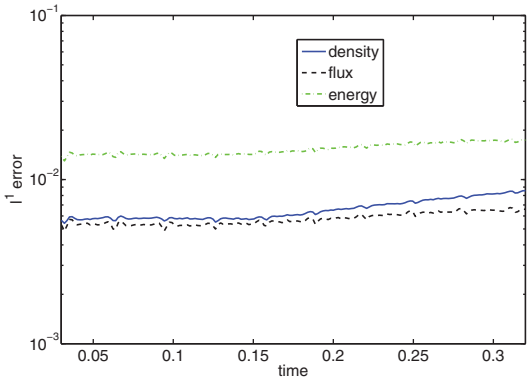

FIG. 4.7. *Comparison of the numerical solution using the AP scheme with the reference solution for the same problem as in Figure* 4.6. *For the first order scheme* (3.2)*, we use* $\Delta t = 0.0016$*,* $\Delta x = 2/128$*. For the reference solution, we use explicit scheme with* $\Delta x = 2/2048$*,* $\Delta t = 2.5e-05$*. Here the x-axis represents time, and we plot the* l^1 *error* (4.14) *for three macroscopic quantities defined in* (4.10).

The singular nature of $s(v, v')$ makes the collision hard to compute numerically, but the cylindrical symmetry of s makes it possible to use polar coordinates so that the singularity in the delta function can be removed and the dimension of the integral can be decreased by one [5, 6, 8]. However, this trick is not easy to implement here since we treat the stiff force term implicitly, and changing to polar coordinates will make it harder to invert. Instead, we use the spectral method [26], which can also remove the singularity.

In this numerical example, assume $d_x = 1$ and $d_v = 2$. Recall that the collision (1.3) can be written as

$$Q = Q^+(f)(t, x, v) - \nu(v) f(t, x, v). \tag{4.16}$$

Similar to [26], we restrict f on the domain $D_v = [-L_v, L_v]^2$ and extend it periodically to the whole domain. L_v is chosen such that the support of f is $\mathrm{supp}(f) \subset B(0, R) = B_R$ and $L_v = 2R$. Approximate f by truncated Fourier series

$$f(v) \approx \sum_{k=-Nv/2+1}^{N_v/2} \hat{f}_k e^{i\frac{\pi}{L_v}k\cdot v}, \qquad \hat{f}_k = \frac{1}{(2L_v)^2}\int_{D_v} f(v) e^{-i\frac{\pi}{L_v}k\cdot v} dv; \tag{4.17}$$

then $Q^+(f)$ is computed as follows:

$$\begin{aligned} Q^+(f) &= \int_{B_R} S(v', v) f(t, x, v') dv' \\ &= \sum_{k=-Nv/2+1}^{N_v/2} \hat{f}_k \int_{B_R} e^{i\frac{\pi}{L_v}k\cdot v'} \left[(n_q + 1) K\delta\left(\frac{1}{2}v^2 - \frac{1}{2}v'^2 + \hbar w_p\right)\right. \\ &\quad \left. + n_q K\delta\left(\frac{1}{2}v^2 - \frac{1}{2}v'^2 - \hbar w_p\right) + K_0\delta\left(\frac{1}{2}v^2 - \frac{1}{2}v'^2\right)\right] dv'. \end{aligned} \tag{4.18}$$

Let $\xi' = \frac{1}{2}v'^2$; then a change of variable $v' = \sqrt{2\xi'}(\cos\theta', \sin\theta')$ leads to

$$\begin{aligned} Q^+(f) = \sum_{k=-Nv/2+1}^{N_v/2} \hat{f}_k \Big[& (n_q+1)K \int_0^{2\pi} e^{i|k|\sqrt{2(\xi+\hbar w_p)}\cos\theta' \frac{\pi}{L_v}} d\theta' \chi_{\xi+\hbar w_p \le \frac{1}{2}R^2} \\ & + n_q K \int_0^{2\pi} e^{i|k|\sqrt{2(\xi-\hbar w_p)}\cos\theta' \frac{\pi}{L_v}} d\theta' \chi_{0\le\xi-\hbar w_p\le\frac{1}{2}R^2} \\ & + K_0 \int_0^{2\pi} e^{i|k|\sqrt{2\xi}\cos\theta' \frac{\pi}{L_v}} d\theta' \chi_{\xi\le\frac{1}{2}R^2} \Big] \\ = \sum_{k=-Nv/2+1}^{N_v/2} & \hat{f}_k B(|k|,|v|) \end{aligned} \tag{4.19}$$

with

$$\begin{aligned} B(|k|,|v|) = 2\pi \Big[& (n_q+1)K J_0\left(\sqrt{2(\xi+\hbar w_p)}|k|\frac{\pi}{L_v}\right)\chi_{\xi+\hbar w_p\le\frac{1}{2}R^2} \\ & + K n_q J_0\left(\sqrt{2(\xi-\hbar w_p)}|k|\frac{\pi}{L_v}\right)\chi_{0\le\xi-\hbar w_p\le\frac{1}{2}R^2} \\ & + K_0 J_0\left(\sqrt{2\xi}|k|\frac{\pi}{L_v}\right)\chi_{\xi\le\frac{1}{2}R^2}\Big], \end{aligned}$$

where J_0 is the Bessel function of order 0

$$J_0(\alpha) = \frac{1}{2\pi}\int_0^{2\pi} e^{i\alpha\cos\theta} d\theta.$$

In the same way, the collision frequency $\nu(v)$ can be computed as

$$\begin{aligned} \nu(v) &= \int_{B(0,L_v)} s(v,v')dv \\ &= 2\pi\left[K(n_q+1)\chi_{0\le\xi-\hbar w_p\le\frac{1}{2}R^2} + K n_q \chi_{\xi+\hbar w_p\le\frac{1}{2}R^2} + K_0\chi_{\xi\le\frac{1}{2}R^2}\right]. \end{aligned} \tag{4.20}$$

Now let $L_v = 8$, $x \in [0,1]$, $K_B T_L = \frac{1}{2}$, $\hbar w_p = 1$, $K = 0$, and $K_0 = 1/5\pi$. Then the two-dimensional Maxwellian is $M = 1/(\sqrt{\frac{\pi}{2K_B T_L}})^2 e^{-\frac{v^2}{2K_B T_L}} = \frac{1}{\pi}e^{-v^2}$. We test two situations. One is for the pure high field regime with fixed $\epsilon = 10^{-3}$ and the initial data taking the form of (4.2) with M replaced by $\frac{1}{\pi}e^{-v^2}$. The macroscopic quantities at time $t = 0.2$ are given in Figure 4.8. The other is for the mixing regimes problem, as ϵ is defined the same as (4.12) but on the space interval $[0,1]$ and initial condition taken as (4.13). To get better accuracy, we use (3.21) and choose $\lambda = \max_v \nu(v)$ in this case, which does not violate the stability constraint. See Figure 4.9 for the time evolution of the macroscopic quantities. The reference solution is calculated by the forward Euler method with the second order slope limiter method for space discretization on a much finer mesh.

It can be checked that the collision frequency (4.20) meets the condition (2.9), but $\phi(v,v') = \frac{s(v,v')}{M(v')}$ does not belong to $W^{1,\infty}(\mathbb{R}^4)$ as assumed in Theorem 2.1. To the authors' knowledge, no result is available numerically or analytically for the existence of the high field limit in this situation. From our numerical experiment, it seems

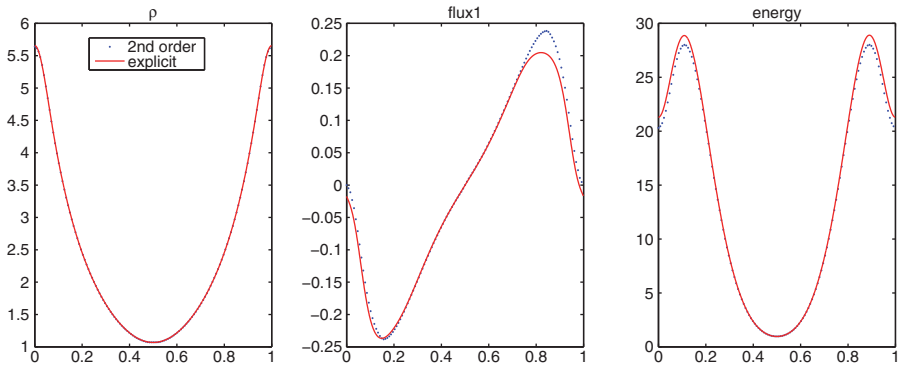

FIG. 4.8. *The macroscopic quantities for the electron-phonon interaction model with smooth initial data* (4.2) *and* $\epsilon = 10^{-3}$*: mass density* (ρ)*, fluxes in* v_1 (*flux*1)*, and* v_2 (*flux*2) *directions, and energy at time* $T = 0.2$*.* $\epsilon = 10^{-3}$*. Solid line: explicit method with* $N_x = 1024$*,* $N_v = 32$*. Dots: second order scheme* (3.21) *with* $N_x = 128$*,* $N_v = 32$*.*

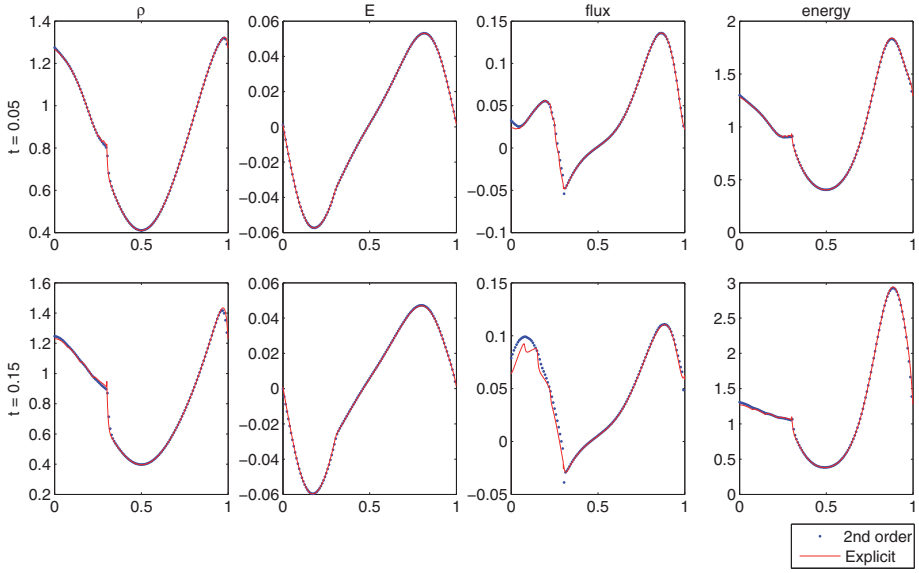

FIG. 4.9. *The time evolution of macroscopic quantities in electron-phonon interaction model in mixing regimes* (4.12) *with initial data* (4.13)*: mass density, electric field, flux in* v_1 *direction, and energy. Solid line: an explicit method with* $N_x = 1024$*,* $N_v = 32$*. Dots: the second order scheme* (3.21) *with* $N_x = 128$*,* $N_v = 32$*.*

to indicate that in this case, the solution does exist since our schemes capture it well in Figure 4.9. This is the first attempt to treat this problem in the high field regime, and we would like to design a fast efficient scheme in the future as well as the approximation of the runaway phenomenon that might be generated in this case.

5. Conclusion. AP numerical schemes for the semiconductor Boltzmann equation efficient in the high field regime have been introduced in this paper. One main difficulty in this problem is that there is no explicit form for the local equilibrium, which is the basic component of the classical AP methods. Our main idea is to penalize the collision term a BGK operator—which is not the local equilibrium of the

high field limit—and treat the stiff force term implicitly by the spectral method. The schemes are designed for both the nondegenerate (isotropic and anisotropic cases) and the degenerate case. We show that these methods have the desired asymptotic properties and can be efficiently implemented with a uniform (in the small parameter) stability. Numerical experiments also demonstrate the accuracy and the correct asymptotic behavior of these schemes.

Acknowledgments. The second author would like to especially thank Dr. Bokai Yan, Prof. Francis Filbet, and Dr. Jingwei Hu for fruitful discussions.

REFERENCES

[1] N. B. Abdallah and H. Chaker, *The high field asymptotics for degenerate semiconductors*, Math. Models Methods Appl. Sci., 11 (2001), pp. 1253–1272.

[2] N. B. Abdallah, H. Chaker, and C. Schmeiser, *The high field asymptotics for a fermionic Boltzmann equation: Entropy solutions and kinetic shock profiles*, J. Hyperbolic Differ. Equ., 4 (2007), pp. 679–704.

[3] N. B. Abdallah and P. Degond, *On a hierarchy of macroscopic models for semiconductors*, J. Math. Phys., 37 (1996), pp. 3306–3333.

[4] N. B. Abdallah, P. Degond, and S. Genieys, *An energy-transport model for semiconductors derived from the Boltzmann equation*, J. Statist. Phys., 84 (1996), pp. 205–231.

[5] J. Carrillo, I. Gamba, A. Majorana, and C. Shu, *A WENO-solver for the* 1*d non-stationary Boltzmann-Poisson system for semiconductor devices*, J. Comput. Electronics, 1 (2002), pp. 365–370.

[6] J. Carrillo, I. Gamba, A. Majorana, and C. Shu, *A WENO-solver for the transients of Boltzmann-Poisson system for semiconductor devices: performance and comparisons with Monte Carlo methods*, J. Comput. Phys., 184 (2003), pp. 498–525.

[7] C. Cercignani, I. M. Gamba, and C. D. Levermore, *High field approximations to a Boltzmann-Poisson system boundary conditions in a semiconductor*, Appl. Math Lett., 10 (1997), pp. 111–118.

[8] Y. Cheng, I. Gamba, A. Majorana, and C. Shu, *Discontinuous Galerkin methods for the Boltzmann-Poisson systems in semiconductor device simulations*, AIP Conf. Proc., 1333 (2011), pp. 890–895.

[9] N. Crouseilles and M. Lemou, *An asymptotic preserving scheme based on a micro-macro decomposition for collisional Vlasov equations: Diffusion and high field scaling limits*, Kinetic and Related Models, 4 (2011), pp. 441–477.

[10] P. Degond, *An Asymptotic Preserving Scheme Based on a Micro-Macro Decomposition for Collisional Vlasov Equations: Diffusion and High-Field Scaling Limits*, AMS/IP Studies in Advanced Mathematics, AMS, Providence, RI, 2000, pp. 77–122.

[11] P. Degond, C. D. Levermore, and C. Schmeiser, *A Note on the Energy-Transport limit of the Semiconductor Boltzmann Equation*, IMA Vol. Math. Appl. 135, Springer, New York, 2004, pp. 137–153.

[12] G. Dimarco and L. Pareschi, *Exponential Runge-Kutta methods for stiff kinetic equations*, SIAM J. Numer. Anal., 49 (2011), pp. 2057–2077.

[13] G. Dimarco and L. Pareschi, *High order asymptotic preserving schemes for the Boltzmann equation*, C.R. Acad. Sci. Ser. I, 350 (2012), pp. 481–486.

[14] F. Filbet, J. Hu, and S. Jin, *A numerical scheme for quantum Boltzmann equation with stiff collision term*, Math. Model Numer. Anal., 46 (2012), pp. 443–463.

[15] F. Filbet and S. Jin, *A class of asymptotic preserving schemes for kinetic equations and related problems with stiff sources*, J. Comput. Phys., 229 (2010), pp. 7625–7648.

[16] G. Frosali and C. V. M. Van der Mee, *Scattering theory relevant to the linear transport of particle swarms*, J. Comput. Phys., 56 (1989), pp. 139–148.

[17] G. Frosali, C. V. M. Van der Mee, and S. L. Paveri-Fontana, *Conditions for runaway phenomena in the kinetic theory of particle swarms*, J. Math. Phys., 30 (1989), pp. 1177–1186.

[18] F. Golse and F. Poupaud, *Limite fluide des equations de Boltzmann des semiconductors pour une statistique de Fermi-Dirac*, Asymptot. Anal., 6 (1992), pp. 135–160.

[19] J. Hu, S. Jin, and B. Yan, *A numerical scheme for the quantum Fokker-Planck-Landau equation efficient in the fluid regime*, Comm. Comput. Phys., 12 (2012), pp. 1541–1561.

[20] C. Jacoboni and P. Lugli, *The Monte Carlo Method for Semiconductor Devices Simulation*, Spring-Verlag, New York, 1989.
[21] S. Jin, *Efficient asymptotic-preserving (AP) schemes for some multiscale kinetic equations*, SIAM J. Sci. Comput., 21 (1999), pp. 441–454.
[22] S. Jin, *Asymptotic preserving (AP) schemes for multiscale kinetic and hyperbolic equations: A review*, Riv. Mat. Univ. Parma, 3 (2012), pp. 177–216.
[23] S. Jin and L. Pareschi, *Discretization of the multiscale semiconductor Boltzmann equation by diffusive relaxation schemes*, J. Comput. Phys., 161 (2000), pp. 312–330.
[24] S. Jin and L. Wang, *An asymptotic preserving scheme for the Vlasov-Poisson-Fokker-Planck system in the high field regime*, Acta Math. Sci., 31 (2011), pp. 2219–2232.
[25] P. Markowich, C. A. Ringhofer, and C. Schmeiser, *Semiconductor Equations*, Springer, New York, 1990.
[26] L. Pareschi and G. Russo, *Numerical solution of the Boltzmann equation* I*: Spectrally accurate approximation of the collision operator*, SIAM J. Numer. Anal., 37 (2000), pp. 1217–1245.
[27] F. Poupaud, *On a system of nonlinear Boltzmann equation of semiconductors physics*, SIAM J. Appl. Math., 50 (1990), pp. 1593–1606.
[28] F. Poupaud, *Diffusion approximation of the linear semiconductor equation: Analysis of boundary layers*, Asymptot. Anal., 4 (1991), pp. 293–317.
[29] F. Poupaud, *Runaway phenomena and fluid approximation under high fields in semiconductor kinetic theory*, Z. Angew. Math. Mech., 72 (1992), pp. 359–372.
[30] R. Stratton, *The influence of interelectron collisions on conduction and breakdown in covalent semiconductors*, Proc. Roy. soc. London Ser. A, 242 (1957), pp. 355–373.
[31] R. Stratton, *Diffusion of hot and cold electrons in semiconductor barriers*, Phys. Rev., 126 (1962), pp. 2002–2014.
[32] B. vanLeer, *Towards the ultimate conservative difference schemes* V*. A second order sequel to Godunov's method*, J. Comput. Phys., 32 (1979), pp. 101–136.
[33] W.V. VanRoosbroeck, *Theory of flow of electrons and holes in Germanium and other semiconductors*, Bell Syst. Techn. J., 29 (1950), pp. 560–607.
[34] B. Yan and S. Jin, *A successive penalty-based asymptotic preserving scheme for kinetic equations*, SIAM J. Sci. Comput., 35 (2013), pp. A150–A172.